



UNIVERSITÀ
DEGLI STUDI
FIRENZE

FLORE

Repository istituzionale dell'Università degli Studi di Firenze

Purification of liquid indium by electric current-induced impurity migration in a static transverse magnetic field

Questa è la Versione finale referata (Post print/Accepted manuscript) della seguente pubblicazione:

Original Citation:

Purification of liquid indium by electric current-induced impurity migration in a static transverse magnetic field / U. Bardi; C. Borri; A. Lavacchi; A. Tolstogouzov; E.B. Trunin; O.E. Trunina. - In: SCRIPTA MATERIALIA. - ISSN 1872-8456. - STAMPA. - 60:(2009), pp. 423-426. [10.1016/j.scriptamat.2008.11.009]

Availability:

This version is available at: 2158/778466 since:

Published version:

DOI: 10.1016/j.scriptamat.2008.11.009

Terms of use:

Open Access

La pubblicazione è resa disponibile sotto le norme e i termini della licenza di deposito, secondo quanto stabilito dalla Policy per l'accesso aperto dell'Università degli Studi di Firenze (<https://www.sba.unifi.it/upload/policy-oa-2016-1.pdf>)

Publisher copyright claim:

(Article begins on next page)

Purification of liquid indium by electric current-induced impurity migration in a static transverse magnetic field

U. Bardi,^a C. Borri,^a A. Lavacchi,^{a,*} A. Tolstogouзов,^a E.B. Trunin^b and O.E. Trunina^b

^aDepartment of Chemistry, University of Firenze, via della Lastruccia 3, 50019 Sesto Fiorentino (FI), Italy

^bInternational Academic Corporation of Science & Culture Ltd., POB 23, 390023 Ryazan, Russian Federation

Received 30 September 2008; revised 12 November 2008; accepted 13 November 2008

Available online 21 November 2008

We have developed an original method for indium purification. Our approach is based on the directional transfer of impurities by applying crossed electric and magnetic fields to the melting volume. The method reduced the concentration of nickel and tin by a factor of 10 while copper was reduced by a factor of 3. A simple hydrodynamic mass transport model describing the process was also derived.

© 2008 Acta Materialia Inc. Published by Elsevier Ltd. All rights reserved.

Keywords: Impurity migration; Indium; Inductively coupled plasma-optical emission spectroscopy (ICP-OES); Purification

Since the late 1980s the demand for, and the price of, indium has increased due to the constant growth of its market [1,2]. High-purity indium is mainly used in the making of indium tin oxide (ITO) thin films for liquid crystal displays (about 65% of the total industrial consumption) and for the production of semiconductor compounds. The required level of the purity here is more than 99.9999 wt.% (6 N quality), i.e. the total concentration of the impurities should be less than 1 part per million (ppm). 6 N indium is produced by a fine purification of primary 4 N metal using different physical and physical-chemical methods (for a review, see Refs. [2,3] and references cited therein) but only physical methods can guarantee minimum contamination by any foreign chemicals or purification plant materials. Traditional crystallization methods such as zone melting and Czochralski crystal growth [4] are also used to achieve a high purification. However, these crystallization methods cannot remove from the solid phase impurities with a unit segregation coefficient, whereas most elements in the concentration range of $10^{-5}\%$ to $10^{-6}\%$ and lower possess such a segregation.

In the present paper, we propose an original approach for a fine purification of indium and other low-melting-point metals. Our method is based on the directional transfer of impurities by applying crossed

electric and magnetic fields [5,6]. We report the construction of our experimental set-up and present the results of the trace element analysis with inductively coupled plasma-optical emission spectroscopy (ICP-OES).

The schematic configuration of our experimental set-up is shown in Figure 1. Liquid indium is moved by the magnetohydrodynamic pump MHDP placed in the pumping zone Z1 via 1.5 mm diameter pipes toward the purification zone Z2, where it passes through the crossed magnetic and electric fields. The static magnetic fields with induction B of 0.6 and 0.5 T in zones Z1 and Z2, respectively, are produced by a set of samarium–cobalt block magnets [7]. The electric currents are provided by 30 A DC power supplies U1, U2 assembled in our laboratory. The electrical connectors k1, k2 equipped with 1.8 mm diameter pure tungsten rods are used to supply power to the liquid metal. All the reservoirs, pipes, pumps and connectors are made of pure Teflon[®] to avoid contamination of the liquid metal. The length of the circuit is 1.5 m, while the length of the purification zone alone is 0.85 m. The system is completely maintained into a Binder heating–drying oven FD 115 [8] with a nominal temperature of 300 °C.

At present, the total amount of indium that can be loaded in our set-up is ~50 g. The refined metal, at least 50% of the initial loading, can be moved off the system simply by switching the pipe to the additional reservoir R2 (Fig. 1) without cooling the metal.

* Corresponding author. Tel.: +39 055 457 3113; fax: +39 055 457 3120; e-mail: alessandro.lavacchi@unifi.it

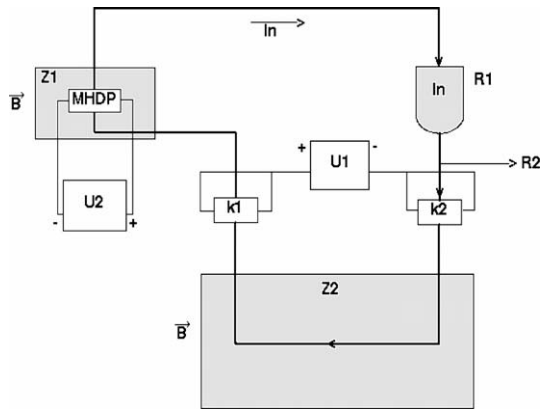


Figure 1. Schematic view of the experimental set-up for indium purification: Z1 is the pumping zone, Z2 is the purification zone, U1 and U2 are the power supplies, k1 and k2 are the connectors, R1 is the reservoir with liquid indium, R2 is the alternative vessel and MHDP is the magnetohydrodynamic pump.

To test our experimental set-up we used 4 N indium manufactured by the Indium Corporation of America [1]. Some physical and thermal properties of indium are listed in Table 1. A 30 h purification experiment was performed at a working temperature of 210 °C with electric currents of 15 and 6 A in the pumping and purification zones, respectively. Under these conditions the average flow rate across the profile of the pipe was of the order of 1 mm s^{-1} , providing 72 complete purification cycles in the experiment. Impurities removed from the melt volume are collected on the pipe wall inside the purification section. The collected impurities do not affect the purification process since the pile up is negligible for the purity of the starting material. The Joule heating for such current densities has been assessed by a finite element numerical approximation of the heat equation as providing temperature increase of less than 2 °C for our experimental conditions, and the effect of this on the melt can be neglected.

ICP-OES measurements were carried out with a standard Perkin-Elmer Optima 2000 DV spectrometer [9,10]. The analytical solutions for ICP-OES were prepared by dissolving 14 mg of indium, collected from

the vessel R1 at different times, in 3 ml of demineralized H_2O with 2 ml of 37% HCl.

In order to check the efficiency of the purification process in the desired concentration range we prepared a model indium sample with a tailored level of impurities (concentration range over 100–200 wt. ppm). To obtain this sample, liquid indium was put in contact with a nickel alloy. By ICP-OES the resulting nickel content in the model sample was estimated as $152.7 \pm 3.1 \text{ ppm}$; further copper and tin were also detected on the level of 0.18 ± 0.01 and $0.17 \pm 0.02 \text{ ppm}$, respectively. We performed the same measurements of the indium samples from the vessel R1 after 20 and 30 h purification cycles. The data are listed in Table 2, as well as the purification coefficient K . The number K is calculated for every kind of impurity as a ratio between the concentrations measured for the as-received sample and after 30 h purification. We have improved the purity of the indium using our approach by a factor of 10 and more with respect to nickel and tin, and more than 3 times for copper impurities. The variation of the purification coefficients with time indicates their dependence on the impurity concentration.

It has been shown [5,6,11–14] that electric current flowing through a liquid metal placed in a static transverse magnetic field produces forces capable of moving the impurities. The most intense of these is the Lorentz force which originates from the local variation of the current densities due to local variation of conductivity. This force can be expressed as:

$$\vec{F} = [\vec{J} \times \vec{B}]V_p \quad (1)$$

where J is the electric current density, B is the magnetic field induction and V_p is the effective impurity volume, which is the region where most of the variations in conductivity occur.

In order to explain the experimental results shown in Table 2, we derived a model aimed at describing the mass transport for the impurities assuming the driving force given by Eq. (1). The model starts from the following assumptions:

- (1) the atoms of the impurities cluster in spherical particles, the radius of which does not depend on the concentration and the effect of the size distribution is negligible;
- (2) no interaction occurs among different impurities;
- (3) the diffusion of impurities is negligible.

The first assumption is strong, but, as shown in Table 2, the concentration dependence vs. time, especially in the case of nickel, is negligible in the considered range.

Table 1. Some physical and thermal properties of indium [1].

Atomic number	49
Molecular weight, g mol^{-1}	114.82
Mass density at 20 °C, g cm^{-3}	7.31
Atomic radius, nm	0.2
Covalent radius, nm	0.144
Ionic radius, nm	0.092
Atomic volume, $\text{cm}^3 \text{ mol}^{-1}$	15.7
Melting point, °C	156.61
Boiling point, °C	2080
Heat of fusion, kJ mol^{-1}	3.27
Heat of vaporization, kJ mol^{-1}	231.8
Heat of atomization, kJ mol^{-1}	243.72
Specific heat, $\text{J g}^{-1} \text{ K}^{-1}$	0.23
Thermal conductivity, $\text{W m}^{-1} \text{ K}^{-1}$	81.6
Electrical resistivity, $\mu\Omega \text{ cm}$	8.37
Dynamic viscosity at 210 °C, Pa s	1.66×10^{-3}

Table 2. Results of ICP-OES trace element analysis of the model indium sample at the initial stage and after 20 and 30 h purification, and purification coefficient $K = C_0/C_{30h}$.

Impurity	Concentration, wt. ppm			K
	Initial sample (C_0)	20 h (C_{20h})	30 h (C_{30h})	
Ni	152.7 ± 3.1	31.4 ± 6.3	15.3 ± 3.1	10
Cu	0.18 ± 0.01	0.05 ± 0.01	0.05 ± 0.01	3.5
Sn	0.17 ± 0.01	0.03 ± 0.01	0.01 ± 0.01	–

These approximations lead to the conclusion that the migration velocity of the particles caused by the Lorentz force does not depend on time; the motion is purely hydrodynamic. So, we can calculate the velocity for each impurity simply by equating the apparent Lorentz force with the viscous drag:

$$V_d = \frac{JV_p B}{6\pi\eta a}, \quad (2)$$

where v_d is the drag velocity of the impurity, η is the dynamic viscosity of the liquid indium at the given temperature and a is the radius of the impurity. The uniform motion combined with the assumption of terminating boundary conditions for the particles hitting the pipe wall, lead to the generic concentration profile shown in Figure 2. The impurity concentration at the end of the purification section is proportional to the dashed area in Figure 2. This area A is given by:

$$A = 2r^2 \arccos\left(\frac{v_d t}{2r}\right) - v_d t \sqrt{\left(r^2 - \left(\frac{v_d t}{2}\right)^2\right)}, \quad (3)$$

where r is the radius of the pipe and t is the time from the start of purification. The average concentration at the end of the purification zone C_f is given by:

$$C_f = \frac{A}{\pi r^2} C_i. \quad (4)$$

In order to calculate the effective concentration averaged on the whole indium volume at a given purification time (T) we have to consider the movement of the indium through the circuit. As the melt exits the purification zone it reaches the reservoir, where it is mixed and again achieves a homogeneous concentration profile. It is also important to note that the volume of the melt in the reservoir is negligible respect to the volume of the pipe. The concentration after the N cycles (the number of cycles in the time T) can be derived according to the following power law relationship:

$$C_T = C_{i0} \left(\frac{C_i}{C_f}\right)^N \quad (5)$$

where C_T is the concentration at time T and C_{i0} is the concentration at purification time $T = 0$. The ratio C_i/C_f is a function of the length and the diameter of the pipe, the electric current, the temperature, the

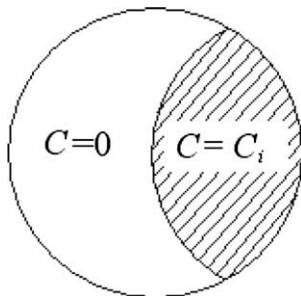


Figure 2. Concentration profile along the purification section. The dashed area is given by the superimposition of the circular cross-section of the pipe with a circle whose center moves with velocity v_d .

applied magnetic field and the physicochemical properties of the melt. The purification coefficient should be related by:

$$K = \frac{C_{i0}}{C_T} \quad (6)$$

Using the values of the purification coefficient for nickel listed in Table 2, we obtained a value of V_p corresponding to that of a sphere with a radius of 4.5 nm; the corresponding value for copper was 3 nm. The value for tin could not be calculated because the final concentration was of the same order of magnitude as the detection limit of the ICP-OES technique.

Diameters for single species are not intended to be taken as corresponding to the existence of a physical sphere showing different concentrations to the average of the bulk. Rather they are to be considered as an effective quantity allowing the use of a simple hydrodynamic model for the complete determination of the mass transport properties of the system. The size of the derived radii also provides the basis for neglecting the contribution from diffusion.

The dynamics of the magnetic transport has probably to be explained in terms of the structure of the liquid alloys. It has been demonstrated that the structure of molten alloys near to the melting point is strongly inhomogeneous in composition. Clustering and medium-range order of the concentration fluctuations occur [15–17]. Such phenomena could explain the inhomogeneous distribution of the current density in the melts. Understanding the structure will also provide an explanation for the deviation from linearity of the purification coefficients which has been assumed here. A quantitative description is in any case still far from being worked out and requires structural information. Such an investigation is planned and will be performed using X-ray diffraction (XRD), small angle X-ray scattering (SAXS) and extended X-ray fine absorption structure (EXAFS).

In conclusion, we have presented an original method and described an experimental set-up for the fine purification of indium and other low-melting-point metals. Our approach, based on the directional transfer of impurities by applying crossed electric and magnetic fields to the melt, improved the purity of as-received indium by a factor of 10 and more with respect to nickel and tin, and by a factor of 3 or more for copper. The ICP-OES data were obtained by collecting samples from the circuit after 30 h of purification performed at a working temperature of 210 °C with electric currents of 15 and 6 A and magnetic induction of 0.6 and 0.5 T applied in the pumping and purification zones, respectively. We described the purification effects in the framework of a simple hydrodynamic model which allowed the effective radius for the inhomogeneities to be estimated. These radii for both nickel and tin have been found to be of the order of several nanometers.

At present, the nature of these large cluster structures is not entirely clear. However, it is evident that common diffusion of individual atoms cannot explain the purification effect observed in our study. A complete understanding of the physics behind the process requires the determination of the structure of the impure indium

melts which will be approached in the future with the use of XRD, SAXS and EXAFS techniques. In the future we will increase the productivity of our machine and move the investigation of our purification process to materials with a higher melting point such as silicon.

This work was supported by ITALBREVETTI Srl. We thank our co-worker B. Cortigiani for assembling the power supplies and technical support, and S. Pucci for performing ICP-OES analysis. We are also very grateful to E. Sentimenti for a gift of 4 N indium.

- [1] <http://www.indium.com>.
- [2] A.M. Alfantazi, R.R. Moskalyk, Minerals Eng. 16 (2003) 687.
- [3] Y. Waseda, M. Isshiki, Purification Process and Characterization of Ultra High Purity Metals, Springer Verlag, Berlin, 2002.
- [4] J.J. Czochralski, Phys. Chem. 14 (1914) 219.
- [5] J. Pratt, R. Sellors, Electrotransport in Metals and Alloys, Trans Tech, Geneva, 1973.
- [6] E.B. Trunin, O.E. Trunina, Inorg. Mat. 39 (2003) 936.
- [7] <http://www.chenyang-ism.com>.
- [8] <http://www.binder-world.com>.
- [9] <http://www.las.perkinelmer.com>.
- [10] J.R. Dean, Practical Inductively Coupled Plasma Spectroscopy, Wiley, Chichester, 2005.
- [11] C. Kittel, Introduction to Solid State Physics, Wiley, New York, 1986, pp. 148.
- [12] H.B. Huntington, A.R. Grone, J. Phys. Chem. Sol. 20 (1961) 76.
- [13] C. Bosvieux, C. Friedel, J. Phys. Chem. Sol. 23 (1962) 123.
- [14] R. Landauer, J.W.F. Woo, Phys. Rev. B 10 (1974) 1266.
- [15] S. Gruner, I. Kaban, R. Kleinhempel, W. Hoyer, P. J v ari, R.G. Delaplane, J. Non-Cryst. Solids 351 (2005) 3490.
- [16] S. Cheng, X. Bian, W. Wang, X. Qin, Physica B 366 (2005) 67.
- [17] J. Hafner, C. Becker, J. Phys.: Condens. Matter 8 (1996) 5269.